Title page

- ***Title***： The effects of humic acid on the toxicity of graphene oxide to *Scenedesmus obliquus* and *Daphnia magna*

- ***Author names and affiliations***:

Ying Zhang*, Tiantian Meng, Liu Shi, Xi Guo, Xiaohui Si, Ruixin Yang, Xie Quan

Laboratory of Industrial Ecology and Environmental Engineering (MOE), School of Environmental Science and Technology, Dalian University of Technology, Dalian 116024, China

Tiantian Meng, E-mail: mengtian0806@mail.dlut.edu.cn

Liu Shi, E-mail: shiliumail@163.com

Xi Guo, E-mail: kathryn@mail.dlut.edu.cn

Xiaohui Si, E-mail: sxh@mail.dlut.edu.cn

Ruixin Yang, E-mail: 18742512482@163.com

Xie Quan, E-mail: xiequan@dlut.edu.cn

- ***Corresponding author:***

Ying Zhang, Ph.D

Laboratory of Industrial Ecology and Environmental Engineering (MOE), School of Environmental Science and Technology, Dalian University of Technology, Dalian 116024, China;

E-mail: yzhang@dlut.edu.cn;

Tel: 86-411-84706252;

Fax: 86-411-84706252

The effects of humic acid on the toxicity of graphene oxide to *Scenedesmus obliquus* and *Daphnia magna*

Abstract

The wide production and application of graphene oxide (GO) has inevitably caused its release to the aquatic ecosystem. However, the influence of natural organic matter (NOM) on the toxicity of GO to aquatic organisms needs further investigation. In this study, we conducted several toxicity tests (i.e., acute toxicity and oxidative damage) with *Scenedesmus obliquus* (*S. obliquus*) and *Daphnia magna* (*D. magna*), as well as a chronic toxicity test with *D. magna*, to investigate the toxicity of GO with or without the presence of humic acid (HA). Our results showed that GO induced significant toxicity to *S. obliquus* and *D. magna*, and the median lethal concentrations (72 h-LC_{50} and 48 h-LC_{50}) for acute toxicity were 20.6 and 84.2 mg L^{-1}, respectively, while the 21 d-LC_{50} for chronic toxicity to *D. magna* was 3.3 mg L^{-1}. Additionally, HA mitigated the acute toxicity of GO to *S. obliquus* and *D. magna* by 28.6% and 32.3%, respectively, and mitigated the chronic toxicity of GO to *D. magna*. In the presence of HA, the decreased toxicity of GO was attributed to the alleviation of oxidative damage by HA to both *S. obliquus* and *D. magna*, the mitigation of surface envelopment to *S. obliquus* and the body accumulation in *D. magna*. Our study provides useful and basic biotoxicity data of GO with a consideration of its interaction with NOM which could aid in preventing an overestimation of the risks of GO to the natural aquatic environment.

Keywords: acute toxicity; chronic toxicity; oxidative damage; surface envelopment; body accumulation

1. Introduction

Graphene, a new class of carbon nanomaterials, is a two-dimensional crystalline material that is composed of a single layer of sp^2 hybridized carbon atoms with a honeycomb-like structure (Pretti *et al.* 2014). Due to its excellent electronic, mechanical, thermal and physicochemical properties, graphene has been used in many areas (e.g., diagnosis, drug delivery systems and cancer therapy) (Nogueira *et al.* 2015). As a functionalized form of graphene, graphene oxide (GO, containing epoxy,

hydroxyl and carboxyl groups) exhibits excellent hydrophilic, biocompatible, mechanical and electrochemical properties, resulting in its extensive application in biotechnology, electronics and other areas (Ruoff & Park 2009; Liu *et al.* 2013). The ubiquitous manufacture and application of GO has made its release to the aqueous environment inevitable.

Although GO has a tendency to aggregate in aqueous suspensions, which consequently make it less available to interact with organisms, it could cause toxicity. GO has been reported to cause acute toxicity to bacteria (Liu *et al.* 2011; Zhang *et al.* 2016), protozoans (Hu *et al.* 2015), zooplankton (Mesarič *et al.* 2013), adult zebrafish (Chen *et al.* 2016) and their embryos (Chen *et al.* 2015; Clemente *et al.* 2017; Zou *et al.* 2018) in the aquatic environment; GO can also as exert effects on oxidative activity within algae and *Euglena gracilis* (Nogueira *et al.* 2015) (Hu *et al.* 2015). Moreover, GO may cause immunotoxicity in adult *Danio rerio* (Chen *et al.* 2016). *Scenedesmus obliquus* (*S. obliquus*) and *Daphnia magna* (*D. magna*), which are the standard organisms for aquatic risk assessment due to their easy cultivation and high sensitivity, have been used to assess the toxicity of nanomaterials such as graphene (Guo *et al.* 2013), carbon nanotubes (Stanley *et al.* 2016) and fullerene (Chen *et al.* 2014). Although there are some reports on the toxicity of GO in *S. obliquus* and *D. magna* (Castro *et al.* 2018), the toxicity mechanism was unclear and needed further investigation to determine the toxicity of GO to aquatic organisms.

Once released into the environment, nanomaterials are subjected to alterations through their interactions with naturally occurring macromolecules, e.g., natural organic matter (NOM). NOM is likely to substantially modify the properties and behaviors of nanomaterial. NOM displaces the weakly bound synthetic capping agents on the nanoparticle surface to form nanoscale coatings, which "masks" the nanoparticles' effects; thus, surface modification could be a major factor that determines the exposure characteristics of nanomaterials. (Lowry *et al.* 2012). The adsorbed NOM macromolecules provide both charge and steric stabilization of nanomaterials, although they may also result in bridging flocculation, so their effects are complex and can be difficult to predict (Lin *et al.* 2017; Park *et al.* 2018). On the other hand, GO is an amphiphile with hydrophilic edges and a more hydrophobic basal plane (Hu *et al.* 2018). The amphiphilic character of GO and the interaction between GO and NOM results in dramatic changes in the aggregation, deposition and toxic properties of GO. Some researchers found that HA has the potential to mitigate the biotoxicity of nanomaterials to the aquatic environment (Chen *et al.*

2014; Chen *et al.* 2015; Zhang *et al.* 2016; Clemente *et al.* 2017). Other researchers have found that the presence of HA increased the colloidal stability of GO and caused an increase in the toxicity of graphene oxide to *D. magna* by affecting their growth rate (Castro *et al.* 2018). The effect of HA on the toxicity of nanomaterials appears unclear and controversial; therefore, further studies on the interactions of nanomaterials with HA should be performed to reduce the uncertainty of the environmental risk assessments that are conducted on nanomaterials.

Here, we conducted a study on GO using several toxicity tests (i.e., acute toxicity, chronic toxicity and oxidative damage tests), with or without the presence of HA. The acute toxicity was characterized by the inhibition of cell growth and chlorophyll-a (Chl-a) synthesis in *S. obliquus* as well as mortality to *D. magna*. The chronic toxicity to *D. magna* was shown by mortality to the parent animals (PA) and the reproductive toxicity to the offspring. The reactive oxygen species (ROS) levels and superoxide dismutase (SOD) and catalase (CAT) activities were used to reflect the oxidative damage that was induced by GO. Furthermore, we also checked the morphology status of *S. obliquus* and body accumulation of *D. magna* with scanning electron microscopy (SEM) and light microscopy to explore the mechanism of toxicity of GO. Our results provide useful and basic biotoxicity data for GO with a consideration of its interaction with NOM, providing an example of how to avoid the overestimation of nanomaterial risks to the natural aquatic environment.

2. Materials and methods

2.1 Materials

GO (thickness: 0.8-1.2 nm; diameter: 0.5-5.0 μm; signal layer ratio: ~99%; purity: >99 wt%), which was synthesized using the classical Hummers' method, was obtained from the Nanjing XFNANO Materials Tech Co., Ltd., China. Humic acid sodium salt was selected as an NOM model due to its solubility in aqueous solution and was purchased from Sigma-Aldrich. Other chemical reagents were of spectral or analytical grade.

GO particles and HA were dispersed in ultrapure water to prepare the stock solution at the final concentrations of 2 g L^{-1} and 1 g L^{-1}, respectively. The stock solutions were sonicated for 30 min before being diluted to different exposure concentrations using the relevant culture medium of *S. obliquus* and *D. magna*, and the components are listed in Table S1 and Table S2.

2.2 Characterization of GO and GO-HA

The size and charge distribution of GO (10 mg L^{-1}) in ultrapure water and the three concentrations of HA (5, 10, 25 mg L^{-1}) were characterized with the Zetasizer Nano analyzer (Nano-ZS90, Malvern, U.K.). Briefly, GO and GO-HA were dissolved in BG-11 medium (pH at 7.5 with sterilization) and ultrapure water, respectively. Next, ultrasonic dispersion was performed for 30 min to measure the diameter and Zeta potential. A UV spectrophotometer (V-560, Jasco, Japan) was used to determine the absorption wavelength of GO and GO-HA in the range of 200-800 nm. A small amount of GO and GO-HA were dissolved in BG-11 medium, dried and analyzed with a Raman spectrometer (DXR, Thermo Fisher, USA) and Fourier-transform infrared spectrometer (FT-IR, 6700, Thermo Fisher, USA) to determine the degree of carbon structure defects and the composition of chemical bonds, respectively.

2.3 Toxicity tests

2.3.1 Culture of test organisms

The algae *S. obliquus* were obtained from the Institute of Hydrobiology of the Chinese Academy of Sciences (Wuhan, China). *S. obliquus* were cultured in an illumination incubator (LRH-250 Gb, Shanghai Bank Equipment, China) at a constant temperature of 25.0 ± 0.5°C with a 12:12 h light-dark cycle and a cool-white fluorescent light intensity of approximately 5000 lx to exponential growth phase. The cultures were shaken three times per day and repositioned within the incubator to minimize any possible illumination and temperature differences and to ensure optimal growth.

D. magna, originally obtained from Dalian Ocean University (Dalian, China), were continuously cultured in our laboratory for more than four years. *D. magna* were fed with *S. obliquus* and were cultured in dechlorinated tap water at a constant temperature of 20 ± 1°C with a 16:8 h light-dark cycle.

2.3.2 Acute toxicity test

The growth inhibition test in *S. obliquus* was performed according to the guideline of OECD 201 (OECD 2006). Algae cells in the exponential growth phase (2×10^5 cell mL^{-1}) were exposed to five concentrations of GO (5, 10, 20, 40 and 80 mg L^{-1}) and one control (BG-11 medium) in a 100 mL test

solution, and tests were performed in triplicate. Then, the cell density of the algae culture was measured at 0 h and 72 h with UV spectrophotometer at 690 nm. The Chl-a content was determined based on ethanol extraction method (Yang *et al.* 2013), and the details of this test are described in our previous study (Ying Zhang 2015).

The acute toxicity test in *D. magna* was performed according to the guideline of OECD 202, (OECD 2004) with some modifications. Five *D. magna* neonates (< 24 h old) were exposed to series of GO concentrations (50.0, 65.0, 84.5, 110.0 and 143.0 mg L^{-1}) and one control (artificial freshwater, AF) in a 50 mL test solution, and the tests were performed in quadruplicate. After this exposure, the 48 h mortality rate was calculated.

2.3.3 Chronic toxicity test

The chronic toxicity test was used to assess the effect of GO and GO-HA on the reproduction of *D. magna*. The test was conducted according to the OECD 211 (OECD 1998) with slight modifications. One *D. magna* neonate (< 24 h old) was exposed to sublethal concentrations of GO at 0, 0.01, 0.1, 1.0, 10, 50 mg L^{-1} in ten replicates. The exposure mediums were renewed every 48 h, and food (*S. obliquus*) was added daily. After 21 d of exposure, the mortality rate of PA, time to produce first brood, offspring number of first brood, offspring number of the most productive brood, and total number of offspring were calculated.

2.3.4 Oxidative damage test

The intracellular ROS content of *S. obliquus* was measured according to Knauert and Knauer (Knauert & Knauer 2008) by using 2',7'-dichlorofluorescin-diacetate (DCFH-DA). Briefly, after the cells were stained with 10 μmol/L DCFH-DA, the fluorescence was measured using a fluorescence spectrophotometer (Thermo Fisher, USA) with the excitation wavelength of 485 nm and emission wavelength of 525 nm. The relative ROS level was represented as the fluorescence intensity ratio of the exposure groups to the control group. SOD and CAT activity assays were performed using commercially available kit (A001-3, A007-1) according to the manufacturer's protocols (Nanjing Jiancheng Bioengineering Institute, China).

The oxidative damage in *D. magna* was measured according to the manufacturer's protocol (Nanjing Jiancheng Bioengineering Institute, China). After exposure, the juvenile *D. magna* (4 d old)

were homogenized in PBS (0.1 M, pH 7.4). The 10% (w/v) supernatant was collected after the homogenate was centrifuged at 10,000 r/min for 10 min (4 ℃), and then the ROS level and the activities of SOD, CAT were analyzed with a commercially available kit (Nanjing Jiancheng Bioengineering Institute, China) in triplicate.

2.4 Scanning electron microscopy (SEM)

For the observation of cell morphology of algae after exposure to GO, samples were centrifuged at 10,000 r/min for 15 min, followed by the removal of the supernatants. The pellets that were obtained after centrifugation were fixed overnight with 2.5% glutaraldehyde and washed with the BG-11 medium three times. Subsequently, the samples were dehydrated in an ethanol gradient (30%, 50%, 70%, 80%, 90%, 95%, and 100%), washed with tert-butyl alcohol and dried under vacuum. The SEM images of algae samples were obtained using SEM (SU8010, Hitachi, Japan).

2.5. Light microscopy observation

The ingestion of GO in the bodies of *D. magna* was observed with a light microscope. After their exposure to GO, the *D. magna* were washed 2 or 3 times with AF and then placed under a light microscope (Model-YS100, Olympus, Japan). The images were visualized through a color-view camera (EOS-760D, Canon, Japan) and analyzed using the AnalySIS software (Soft Imaging System, USA).

2.6 Statistical analysis

All statistical analyses were conducted with Origin 8.0 (Origin Lab, USA) and SPSS 18.0 (IBM, USA). The data shown in this study are expressed as the mean ± SD unless otherwise specified. A one-way ANOVA with Tukey's test ($p < 0.05$) was used to test for a significant difference.

3. Results

3.1 Characteristics of GO and GO-HA

Physicochemical properties are important parameters that influence the toxicity of nanomaterials, so the particle size, Zeta potential, absorption wavelength, carbon structures and chemical bond compositions of the GO and GO-HA samples were analyzed. As shown in **Table 1**, the size of GO in

ultrapure water is 1108 nm and decreases to 405 nm when the concentration of HA is 25 mg L^{-1}. The Zeta potential of GO increased from -31.7 mV to -41.5 mV with an increasing concentration of HA (**Table 1**). The change in the particle size and Zeta potential of GO in different concentrations of HA suspensions indicated that HA could reduce the agglomeration of GO by promoting better dispersion. The UV-Vis absorption spectroscopy showed that GO and GO-HA exhibited a strong absorption band that was centered at 227 nm, suggesting that HA did not change the absorption band of GO (**Fig. S1a**). In **Fig. S1b**, the Raman spectra of GO and GO-HA show that the intensity ratio of the D band to the G band decreased from 1.02 to 0.97 in the presence of HA, suggesting that HA decreased the disordered structure of GO. The FT-IR spectra of GO and GO-HA comprised bands at 3430, 2975, 1618, and 1048 cm^{-1}, which were attributed to the stretching vibrations of O-H, C-H, C=O and C-O, while the peak at 1398 cm^{-1} was ascribed to the deformation vibration of CH_3 (**Fig. S1c**).

Table 1 The size and Zeta potential of GO in different suspensions

Suspensions	Ultrapure water	HA (mg/L)		
		5	10	25
Size (nm)	1108 ± 51	960 ± 214	755 ± 153	405 ± 12
Zeta potential (mV)	-31.7 ± 2.9	-35.1 ± 2.7	-39 ± 1.7	-41.5 ± 0.8

3.2 Effect of HA on acute toxicity induced by GO

The effect of HA (0, 5, 10, 25 mg L^{-1}) on the acute toxicity of GO to *S. obliquus* and *D. magna* is shown in **Fig. 1**. **Fig. 1**A and **Fig. 1**B show that both the cell growth inhibition rate and Chl-a synthesis inhibition rate of *S. obliquus* increased with the concentration of GO, and the inhibition rate decreased significantly in a concentration-dependent manner when HA was present. As shown in **Fig. 1**C, the 48 h exposure to GO induces significant mortality in *D. magna*, while the addition of HA significantly mitigates the mortality rate.

The median value of the lethal concentration (LC_{50}) of *S. obliquus* after a 72 h exposure to GO increased from 20.6 to 26.5 mg L^{-1} (by 28.6%) in the presence of HA (**Table 2**), indicating that HA could reduce the acute toxicity of GO to *S. obliquus* in a concentration-dependent manner. The 48 h-LC_{50} of *D. magna* increased from 84.3 to 111.4 mg L^{-1} in the presence of HA (**Table 2**), where the mitigation rate reached 32.3%. Therefore, both the results suggested that HA could significantly

191 mitigate the acute toxicity of GO to *S. obliquus* and *D. magna*.

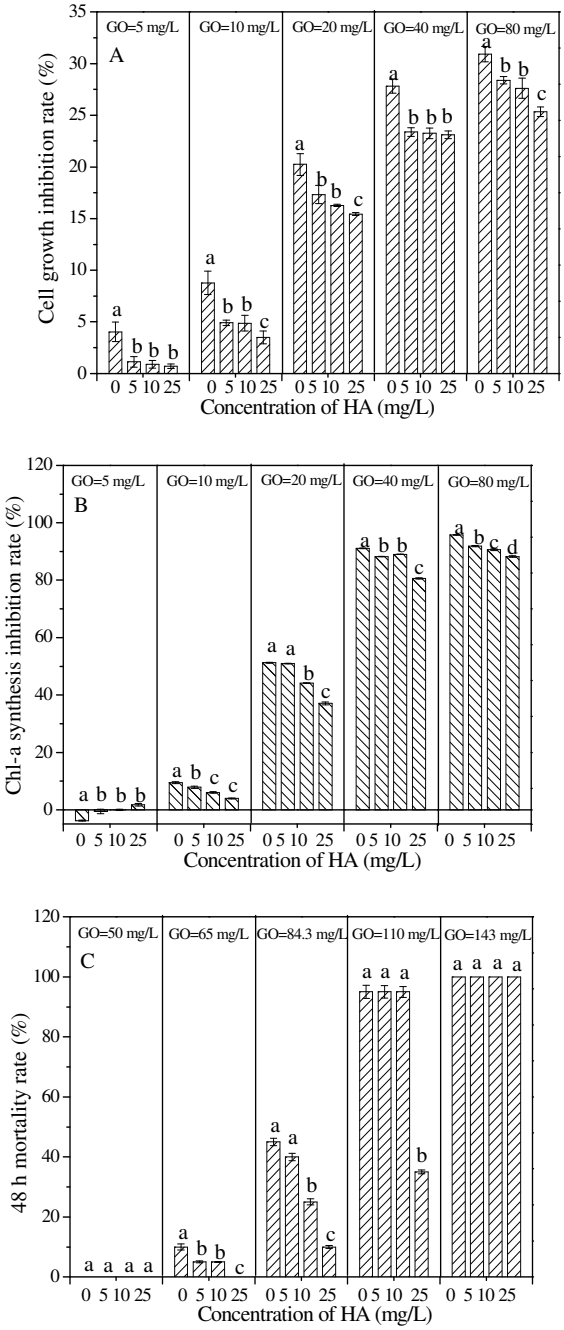

192

193

194

195 **Fig. 1**. The effect of HA on acute toxicity to *S. obliquus* and *D. magna* that was induced by GO.

196 Note: (A) Cell growth inhibition rate and (B) Chl-a synthesis inhibition rate in *S. obliquus*; (C) 48 h mortality rate in *D.*

197 *magna*. The different letters above the columns denote significant differences at $p < 0.05$.

198

199 **Table 2** The effect of different HA concentrations on the LC_{50} values of GO in *S. obliquus* and *D. magna*

HA concentrations	*S. obliquus*	*D. magna*
(mg L^{-1})	LC_{50} (mg L^{-1})	

0	20.6	84.3
5	21.8	87.7
10	23.5	90.4
25	26.5	111.4

3.3 Effect of HA on chronic toxicity induced by GO

Based on the investigation of the acute toxicity of GO, we conducted chronic toxicity tests (21 d mortality test and reproduction test) with *D. magna*, and the results are given in **Fig. 2**. As shown in **Fig. 2**A, the 21 d mortality rate of PA increased gradually from 0 to 100% when the GO concentration increased from 0.01 mg L^{-1} to 50 mg L^{-1}, which suggested that the 21 d mortality rate of *D. magna* was concentration-dependent with GO. When HA was present, the 21 d mortality rate of PA decreased significantly, with the 21 d-LC_{50} increasing from 3.3 mg L^{-1} to 9.7 mg L^{-1} (**Fig. 2**A), suggesting that HA could mitigate the mortality rate of PA. The results of the reproductive toxicity tests are given in **Fig. 2** (B-E). It can be seen from **Fig. 2**B that the time to produce the first brood gradually increased with increasing concentrations of GO, and the first brood was not found in the experimental period of 21 d at GO concentration ≥ 10 mg L^{-1}. However, the presence of HA significantly reduced the time to the produce first brood compared exposure to GO. The offspring number of the first brood, offspring number of the most productive brood and total number of offspring also gradually decreased with the increasing concentrations of GO in a concentration-dependent manner (**Fig. 2**C-E). When HA was present, the production of neonates was increased compared with treatment with GO alone at the same concentration of GO (**Fig. 2**C-E), suggesting that HA could significantly mitigate the reproductive toxicity of GO to *D. magna*.

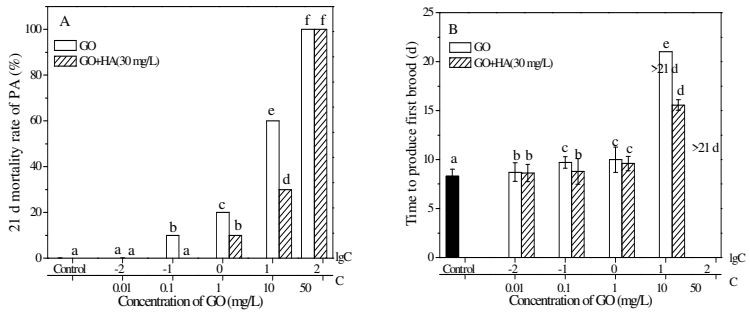

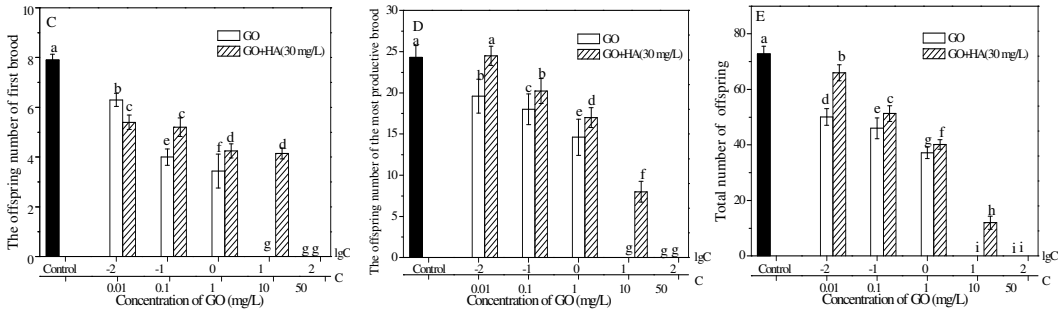

Fig. 2. Effect of HA on chronic toxicity to *D. magna* induced by GO.

Note: (A) 21 d mortality rate of PA, (B) Time to produce first brood, (C) The offspring number of first brood, (D) The offspring number of the most productive brood, (E) Total number of offspring. The different letters above the columns denote significant differences at $p < 0.05$.

3.4 Effect of HA on oxidative damage induced by GO

In order to explore the effect of HA (0, 5, 10, 25 mg L^{-1}) on oxidative damage induced by GO, we conducted toxicity tests with *S. obliquus* and *D. magna*. Additionally, the ROS level and SOD and CAT activities were used to reflect the mechanisms of toxicity in *S. obliquus* and *D. magna* (**Fig. 3**).

As shown in **Fig. 3**A, the ROS level of *S. obliquus* was increased significantly after exposure to GO (20 mg L^{-1}) for 72 h, indicating that GO could damage the oxidative system of *S. obliquus*. The relative ROS level was decreased significantly with the addition of HA in a concentration-dependent manner, which suggested that HA could mitigate the high levels of oxidative stress that were induced by GO in *S. obliquus*. After exposure to GO, the SOD and CAT activities of *S. obliquus* were also increased in a similar pattern to that of ROS (**Fig. 3**B and **Fig. 3C**). Compared with the GO exposure group, the SOD and CAT activities were gradually decreased with increasing concentrations of HA. This result indicated that the defensive ability of the antioxidant system to remove hydrogen peroxide radicals and superoxide anion radicals was reduced, reflecting the possibility that HA mitigated the oxidative damaged that was induced by GO.

As shown in **Fig. 3D**, GO (10 mg L^{-1}) exposure significantly promoted the generation of ROS in *D. magna*. The relative ROS level reached 136% compared with the control, and the ROS content decreased with the presence of HA. This result suggested that the oxidative damage of GO to *D. magna* was mitigated with the coadministration of HA. GO exposure also enhanced the activities of SOD and CAT in *D. magna*, especially the CAT activity, which increased by more than twofold compared with the control (**Fig. 3**E and **Fig. 3**F). An increase in the HA concentration resulted in

significant decreases in the SOD and CAT activities, suggesting that HA could mitigate the oxidative damage to *D. magna* that was induced by GO.

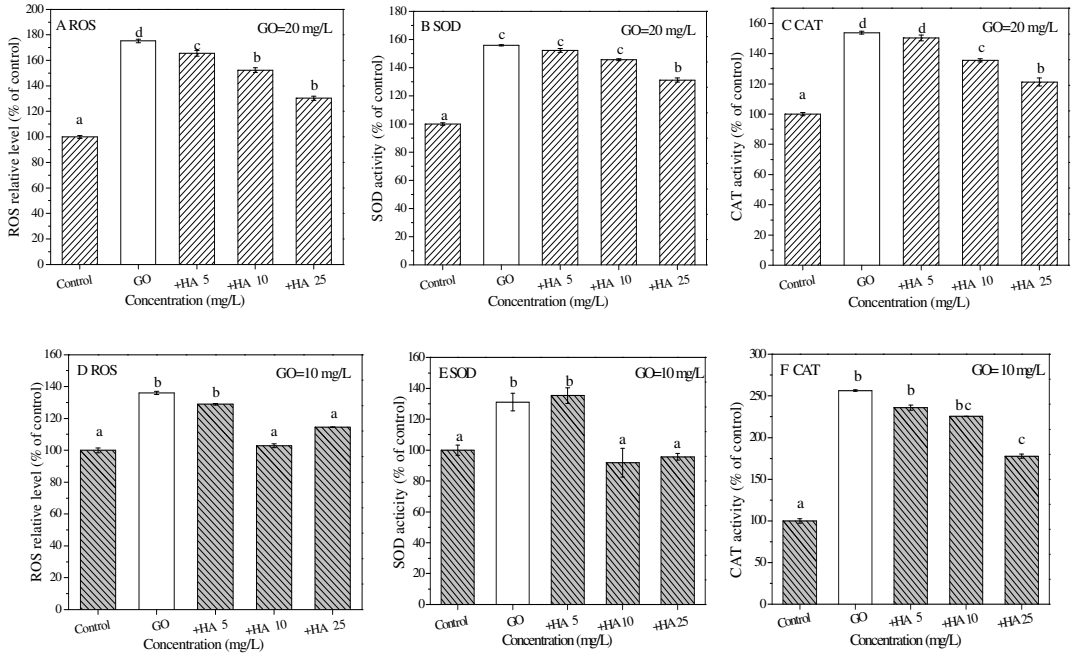

Fig. 3. The effect of HA on oxidative damage that was induced by GO in *S. obliquus* and *D. magna*.

Note: (A) ROS relative level, (B) SOD activity and (C) CAT activity of *S. obliquus*; (D) ROS relative level, (E) SOD activity and (F) CAT activity of *D. magna*. The different letters above columns denote significant differences at $p < 0.05$.

3.5 Effect of HA on surface morphology alterations induced by GO in *S. obliquus*

To clarify the impact of HA on the morphological alterations that were induced by GO in *S. obliquus*, we applied SEM to evaluate the cellular surface of *S. obliquus* after exposure to GO for 72 h. As shown in **Fig. 4**, the cells in the control group were intact without morphological damage and had uniform diameters of approximately 2 μm. However, there were apparent shrinkages in the cell surfaces after exposure to GO and GO-HA, indicating that the cell morphology was damaged considerably. Furthermore, the cells surface was enveloped with nanomaterial in the GO exposure groups (as denoted by the black circles), while the envelopment was markedly reduced in the GO-HA exposure groups (as denoted by the black arrows), which suggested that HA could reduce the agglomeration of GO on the cell surface and mitigate the physical damage that was induced by GO.

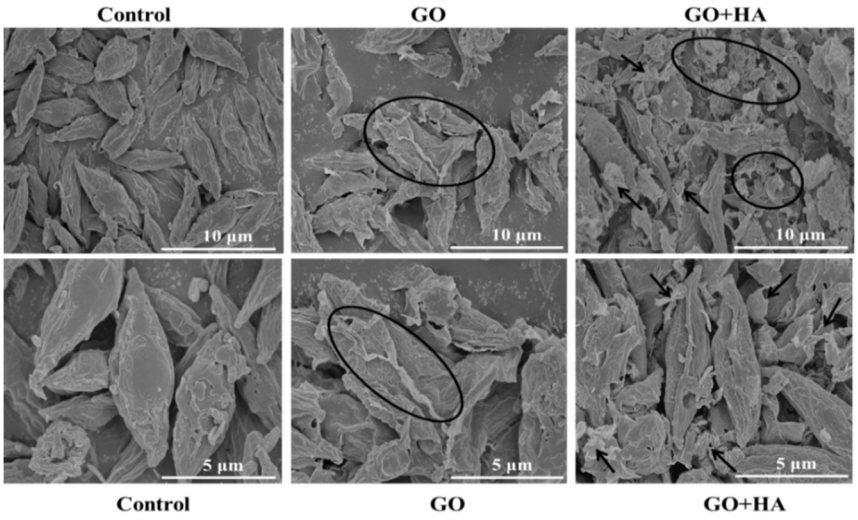

Fig. 4. SEM images of algae cells exposed to GO with or without HA.

Note: Black arrows indicate the scattered debris of nanomaterials; black circles indicate the envelopment of cells by the nanomaterials.

3.6 Effect of HA on the accumulation of GO in *D. magna*

The accumulation of GO in the body of *D. magna* was investigated at 48 h and 21 d, and the results are shown in **Fig. 5**. As shown in **Fig. 5**A, that there was a dark brown accumulation in the digestive tract of *D. magna* after 48 h GO exposure (as denoted by arrows), indicating that GO could be swallowed directly by the *D. magna* and that it accumulated in the digestive tract. The addition of HA (30 mg L^{-1}) mitigated the accumulation of GO in the digestive tract (**Fig. 5**A), indicating that HA could contribute to the excretion of GO. After the 21 d exposure, the accumulation of GO in the digestive tract of *D. magna* (as denoted by arrows) was still observed; meanwhile, the number of offspring decreased with the increased concentrations of GO (**Fig. 5**B). This indicated that the uptake of GO was a long-term process, which in turn affected the reproduction of *D. magna*. Compared with the GO exposure groups, the accumulation of GO in *D. magna* decreased remarkably in the presence of HA, and the number of offspring increased considerably, suggesting that the presence of HA could accelerate the excretion of GO and then mitigate the reproductive toxicity of GO.

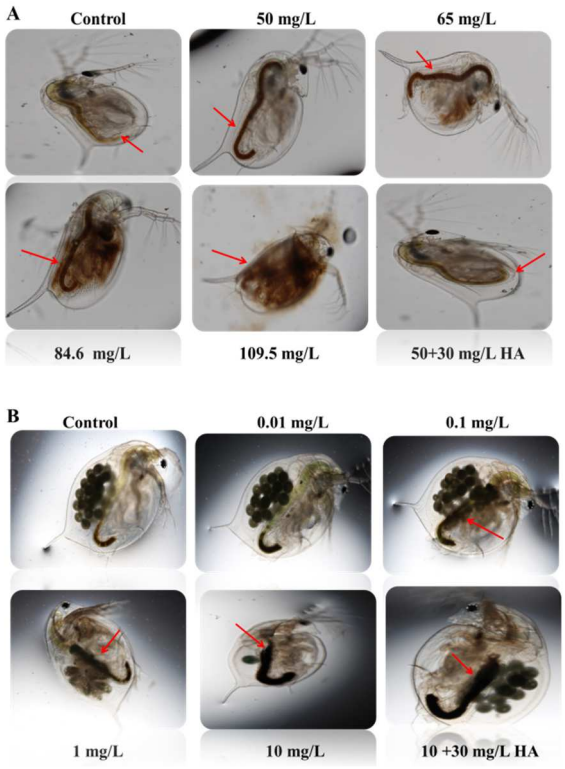

Fig. 5. Effect of HA on the accumulation of GO in *D. magna*.

Note: (A) Effect of HA on the accumulation of GO in *D. magna* after a 48 h exposure; (B) Effect of HA on the accumulation of GO in *D. magna* after a 21 d exposure.

4 Discussion

To investigate the toxic effects of GO on aquatic organisms, we conducted multiple tests of toxicity (i.e., acute toxicity, chronic toxicity and oxidative damage) with *S. obliquus* and *D. magna*. In the case of acute toxicity, the 72 h-EC_{50} and 48 h-EC_{50} of *S. obliquus* and *D. magna* were calculated to be 20.6 and 84.2 mg L^{-1}, indicating that *S. obliquus* was more sensitive to the toxicity of GO than *D. magna*. Other researchers have reported a similar EC_{50} of GO; e.g., Nogueira et al. reported that GO was toxic to algae, (*Raphidocelis subcapitata*) with a 96 h-EC_{50} of 20 mg L^{-1} (Nogueira *et al.* 2015), and Zhao et al. reported that the 96-h EC_{50} of GO algae (*Chlorella pyrenoidosa*) was 37 mg L^{-1} (Zhao *et al.* 2017b). As for the toxicity of GO to *D. magna*, Lv et al. reported that the 72 h- LC50 was 45.4 mg L^{-1} (Lv *et al.* 2018), while the 48 h-EC50 was reported to be 150.75 mg L^{-1} (Liu *et al.* 2018a). Our results lay in the range of the reported values of toxicity data, which confirmed the substantial toxicity of GO and supplemented the more basic data on GO toxicity to include more aquatic organisms.

In addition to acute toxicity, chronic toxicity studies should also receive adequate attention in the

conduction of a potential risk assessment of nanomaterials (Arndt *et al.* 2013). The concentration of GO in the environment is reported to be approximately 0.01-1 mg L^{-1} (Mendonca *et al.* 2011; Seda *et al.* 2012; Souza *et al.* 2018); this low environmental concentration of GO did not exhibit acute lethal toxicity to *D. magna* in our study. However, the chronic toxicity test after 21 d reflected that GO exposure could cause adverse effects on the reproduction of *D. magna* (e.g., the time to produce first brood and the number of offspring), or even cause the death of PA at this low concentration. Our results were consistent with other studies showing that GO caused a significant decrease in the number of neonates after a long-term exposure when its concentration was ≥ 0.4 mg L^{-1} (Mendonca *et al.* 2011; Seda *et al.* 2012; Liu *et al.* 2018b; Souza *et al.* 2018). Mendonca et al. and Seda et al. reported that C_{70}-GA and diamond nanomaterials could also induce chronic toxicity to *D. magna* even at very low concentrations. Thus, chronic toxicity tests are required and necessary for risk considerations of long-term exposures.

The effect of HA on the toxicity of GO was further investigated in our study, which could reflect the substantial toxicity of GO when it is released to the natural environment. At the level of acute toxicity, we found that HA could mitigate the acute toxicity of GO to *S. obliquus* and *D. magna* in a concentration-dependent manner (see **Fig. 1**). Similar results have reported that HA mitigated the toxicity of G and GO to zebrafish embryos, *Escherichia coli* and wheat (Hu *et al.* 2014; Chen *et al.* 2015; Zhang *et al.* 2016). From the mitigation rates of acute toxicity to *S. obliquus* and *D. magna*, we concluded that effect of HA on the mitigation of acute toxicity in *D. magna* was more obvious than in *S. obliquus*, which may be attributable to the interaction of HA with the enhanced excretion ability of *D. magna*. This phenomenon was also found by Chen et al., who noted that HA did reduce the uptake and accelerated the depuration of fullerene in *D. magna* (Chen *et al.* 2014). The addition of HA also mitigated the chronic toxicity of GO to *D. magna*, as shown by the results of PA mortality and reproductive toxicity. As we know, our study is the first report to reflect the influence of HA on the chronic toxicity of GO in Daphnia, providing useful information for the chronic toxicity data of GO. In conclusion, more attention should be given to the influence of HA on the biotoxicity of GO to avoid an overestimation of the risk of GO in water in nature.

The toxicity mechanisms of GO were explored from the following aspects in our study: surface envelopment, oxidative damage and body accumulation. We found that oxidative damage was a

common mechanism of GO toxicity in *S. obliquus* and *D. magna*. When *S. obliquus* and *D. magna* were exposed to GO, both of their cellular ROS levels (such as $O_2^{\bullet-}$ and H_2O_2) increased significantly. In general, the antioxidant enzymes (such as SOD and CAT) can specifically catalyze $O_2^{\bullet-}$ and H_2O_2 into O_2 and H_2O, thus maintaining ROS at a relatively stable level and protecting organisms from damage by excessive ROS (Hu *et al.* 2015). Therefore, the cellular antioxidant enzymes are regarded as the sensitive biomarkers for various environmental stresses. In the present study, the increased activities of SOD and CAT indicated an enhanced ability of *S. obliquus* and *D. magna* to scavenge the $O_2^{\bullet-}$ and H_2O_2 radicals, which suggesting that GO induced excessive ROS and caused damage to the oxidative system. Accordingly, we considered that oxidative damage could be the common pathway that contributed to the toxicity of GO to *S. obliquus* and *D. magna*. In the presence of HA, we found that the ROS level decreased significantly (**Fig. 3**), which reflected the actions of HA as a free radical scavenger to reduce the oxidative damage of GO to *S. obliquus* and *D. magna*. Similar results were also reported on zebrafish embryos and *Escherichia coli* where HA reduced the oxidative damage of GO (Chen *et al.* 2015; Zhang *et al.* 2016; Clemente *et al.* 2017). Therefore, we concluded that the presence of HA could mitigate the oxidative damage to *S. obliquus* and *D. magna* that was caused by GO.

From the morphology alterations of *S. obliquus,* we found that surface envelopment was also one of the contributors to the toxicity of GO. SEM images showed that nanoscale GO covered the cell surfaces, resulting in obvious ruffles on the cells after exposure to GO for 72 h. This physical envelopment has also reported in other studies that demonstrate that reduced graphene oxide, GO and graphene could cause the destruction of the cellular structures of algae (Du *et al.* 2016; Zhao *et al.* 2017a). Accordingly, we considered that the surface envelopment could be one of the possible toxicity mechanisms of GO to *S. obliquus*. In the presence of HA, we found that the envelopment of GO on cell surfaces was mitigated. This suggested that HA could mitigate the agglomeration of GO in aquatic solutions, which was confirmed by the decreased particle sizes and increased Zeta potentials of GO in the presence of HA (**Table 1**). Chen et al. addressed that the increase in Zeta potentials could minimize the toxicity of nanomaterials by charge repulsion, and our results were consistent with their studies that HA alleviated the toxicity of GO by increasing its surface negative charges (Shim *et al.* 2014; Chen *et al.* 2015). Therefore, we speculated that the regulation of Zeta potential and particle

size with the HA presence could contribute to the mitigation of surface envelopment caused by GO.

Considering the interior influence of GO to *D. magna,* we found that the body accumulation of GO may also contribute to its toxicity. The light microscopy images showed that GO accumulated in the gut of *D. magna* after exposure to GO for 48 h and 21 d (**Fig. 5**). *D. magna*, as a filter-feeding creature, can ingest substances with a diameter of 0.4-4 μm in water (Baun *et al.* 2008). The average particle size of GO in the ultrapure water that was used in our study is 1108 nm (approximately 1 μm), so it is capable of being directly swallowed by *D. magna*. The GO that is swallowed tends to accumulate and block the digestive tract, preventing the normal feeding of *D. magna* and decreasing the number of offspring, even leading to death.

The tendency of GO and other nanomaterials to accumulate in the body of *D. magna* due to their small size was also evidenced by other studies (Guo *et al.* 2013; Mesaric *et al.* 2015; Stanley *et al.* 2016; Lv *et al.* 2018). Some studies reported that *D. magna* could excrete the accumulated nanomaterials from the body in the case of feeding (Guo *et al.* 2013). However, complete excretion did not occur, as some carbon nanomaterials still remained in its body (Elijah J. Petersen *et al.* 2010). Therefore, we speculated that the obstruction of the digestive tract would be one of the possible toxicity routes of GO to *D. magna* based on our results in **Fig. 5**. We also found that the accumulated nanomaterials decreased remarkably with the presence of HA. Chen et al. reported that the ingestion of nanomaterials could be reduced with the increased Zeta potential (Chen *et al.* 2014). The electronegativity of GO was enhanced with the presence of HA in our study, which suggested that the enhanced of Zeta potential may be one contributor to the decrease of accumulated GO in *D. magna*. Meanwhile, the decreased size of GO in the presence of HA may also contribute to the reduction of accumulated GO in *D. magna*, since it was considered that the nanomaterials with a small size were easily excreted by *D. magna* (Chen *et al.* 2014). Therefore, we speculated that both the regulation of Zeta potential and particle size when HA was present were the main contributors to the mitigation of accumulated GO in the body of *D. magna*.

5 Conclusion

In this study, we systematically investigated the multilevel toxicity (acute toxicity, chronic toxicity, and oxidative damage) of GO to *S. obliquus* and *D. magna*, as well as the effect of HA coexposure on their toxicities. Our results showed that *S. obliquus* was more sensitive to the toxicity of GO than *D. magna*. HA could significantly mitigate the acute toxicity and oxidative damage of GO to *S. obliquus* and *D. magna* as well as alleviate the chronic toxicity of GO to *D. magna.* HA could also mitigate the surface envelopment in *S. obliquus* and decrease the accumulation of GO in the body of *D. magna*. Our findings aid in understanding the biotoxicity and ecological risks of GO with the consideration of its potential interaction with NOM, avoiding an overestimation of the risks of GO in the natural aquatic environment.

Refrences

Arndt, D.A., Moua, M., Chen, J. & Klaper, R.D. (2013). Core structure and surface functionalization of carbon nanomaterials alter impacts to daphnid mortality, reproduction, and growth: acute assays do not predict chronic exposure impacts. *Environ Sci Technol*, 47, 9444-9452.

Baun, A., Hartmann, N.B., Grieger, K. & Kusk, K.O. (2008). Ecotoxicity of engineered nanoparticles to aquatic invertebrates: a brief review and recommendations for future toxicity testing. *Ecotoxicology*, 17, 387-395.

Castro, V.L., Clemente, Z., Jonsson, C., Silva, M., Vallim, J.H., de Medeiros, A.M.Z. *et al.* (2018). Nanoecotoxicity assessment of graphene oxide and its relationship with humic acid. *Environ Toxicol Chem*, 37, 1998-2012.

Chen, M.J., Yin, J.F., Liang, Y., Yuan, S.P., Wang, F.B., Song, M.Y. *et al.* (2016). Oxidative stress and immunotoxicity induced by graphene oxide in zebrafish. *Aquatic Toxicology*, 174, 54-60.

Chen, Q., Yin, D., Li, J. & Hu, X. (2014). The effects of humic acid on the uptake and depuration of fullerene aqueous suspensions in two aquatic organisms. *Environ Toxicol Chem*, 33, 1090-1097.

406 Chen, Y., Ren, C., Ouyang, S., Hu, X. & Zhou, Q. (2015). Mitigation in Multiple Effects of Graphene
407 Oxide Toxicity in Zebrafish Embryogenesis Driven by Humic Acid. *Environ Sci Technol*, 49,
408 10147-10154.
409 Clemente, Z., Castro, V.L.S.S., Franqui, L.S., Silva, C.A. & Martinez, D.S.T. (2017). Nanotoxicity of
410 graphene oxide: Assessing the influence of oxidation debris in the presence of humic acid.
411 *Environmental pollution*, 225, 118-128.
412 Du, S., Zhang, P., Zhang, R., Lu, Q., Liu, L., Bao, X. *et al.* (2016). Reduced graphene oxide induces
413 cytotoxicity and inhibits photosynthetic performance of the green alga Scenedesmus obliquus.
414 *Chemosphere*, 164, 499-507.
415 Elijah J. Petersen, Roger A. Pinto, Danielle J. Mai, Peter F. Landrum & Walter J. Weber, J.R. (2010).
416 Influence of polyethyleneimine graftings of multi-walled carbon nanotubes on their
417 accumulation and elimination by and toxicity to Daphnia magna. *Environmental science &*
418 *technology*, 45, 1133-1138.
419 Guo, X.K., Dong, S.P., Petersen, E.J., Gao, S.X., Huang, Q.G. & Mao, L. (2013). Biological Uptake
420 and Depuration of Radio-labeled Graphene by Daphnia magna. *Environmental Science &*
421 *Technology*, 47, 12524-12531.
422 Hu, C., Wang, Q., Zhao, H., Wang, L., Guo, S. & Li, X. (2015). Ecotoxicological effects of graphene
423 oxide on the protozoan Euglena gracilis. *Chemosphere*, 128, 184-190.
424 Hu, X., Mu, L., Kang, J., Lu, K., Zhou, R. & Zhou, Q. (2014). Humic acid acts as a natural antidote of
425 graphene by regulating nanomaterial translocation and metabolic fluxes in vivo *Environ Sci*
426 *Technol*, 48, 6919-6927.
427 Hu, X.G., Ren, C.X., Kang, W.L., Mu, L., Liu, X.W., Li, X.K. *et al.* (2018). Characterization and
428 toxicity of nanoscale fragments in wastewater treatment plant effluent. *Sci Total Environ*, 626,
429 1332-1341.
430 Knauert, S. & Knauer, K. (2008). The Role of Reactive Oxygen Species in Copper Toxicity to Two
431 Freshwater Green Algae. *Journal of Phycology*, 44, 311-319.
432 Lin, S.J., Wang, H.T. & Yu, T.Y. (2017). A promising trend for nano-EHS research - Integrating fate
433 and transport analysis with safety assessment using model organisms. *Nanoimpact*, 7, 1-6.

Liu, J., Cui, L. & Losic, D. (2013). Graphene and graphene oxide as new nanocarriers for drug delivery applications. *Acta Biomaterialia*, 9, 9243.

Liu, S., Zeng, T.H., Hofmann, M., Burcombe, E., Wei, J., Jiang, R. *et al.* (2011). Antibacterial activity of graphite, graphite oxide, graphene oxide, and reduced graphene oxide: membrane and oxidative stress. *Acs Nano*, 5, 6971-6980.

Liu, Y.Y., Fan, W.H., Xu, Z.Z., Peng, W.H. & Luo, S.L. (2018a). Comparative effects of graphene and graphene oxide on copper toxicity to &ITDaphnia magna&IT: Role of surface oxygenic functional groups. *Environ Pollut*, 236, 962-970.

Liu, Y.Y., Han, W.L., Xu, Z.Z., Fan, W.H., Peng, W.H. & Luo, S.L. (2018b). Comparative toxicity of pristine graphene oxide and its carboxyl, imidazole or polyethylene glycol functionalized products to Daphnia magna: A two generation study. *Environ Pollut*, 237, 218-227.

Lowry, G.V., Gregory, K.B., Apte, S.C. & Lead, J.R. (2012). Transformations of Nanomaterials in the Environment. *Environ Sci Technol*, 46, 6893-6899.

Lv, X.H., Yang, Y., Tao, Y., Jiang, Y.L., Chen, B.Y., Zhu, X.S. *et al.* (2018). A mechanism study on toxicity of graphene oxide to Daphnia magna: Direct link between bioaccumulation and oxidative stress. *Environ Pollut*, 234, 953-959.

Mendonca, E., Diniz, M., Silva, L., Peres, I., Castro, L., Correia, J.B. *et al.* (2011). Effects of diamond nanoparticle exposure on the internal structure and reproduction of Daphnia magna. *J Hazard Mater*, 186, 265-271.

Mesaric, T., Gambardella, C., Milivojevic, T., Faimali, M., Drobne, D., Falugi, C. *et al.* (2015). High surface adsorption properties of carbon-based nanomaterials are responsible for mortality, swimming inhibition, and biochemical responses in Artemia salina larvae. *Aquatic Toxicology*, 163, 121-129.

Mesarič, T., Sepčič, K., Piazza, V., Gambardella, C., Garaventa, F., Drobne, D. *et al.* (2013). Effects of nano carbon black and single-layer graphene oxide on settlement, survival and swimming behaviour of Amphibalanus amphitritelarvae. *Chemistry and Ecology*, 29, 643-652.

Nogueira, P.F., Nakabayashi, D. & Zucolotto, V. (2015). The effects of graphene oxide on green algae Raphidocelis subcapitata. *Aquat Toxicol*, 166, 29-35.

462 OECD (1998). Organization for Economic Cooperation and Development (OECD). 211. Guideline
463 for Testing of Chemicals, Daphnia Magna Reproduction Test.
464 OECD (2004). OECD 202
465 Organization for Economic Cooperation and Development (OECD). 202. Guideline for the Testing of
466 Chemicals, Daphnia sp., Acute Immbilisation Test.
467 OECD (2006). Organization for Economic Cooperation and Development (OECD). Guidelines for the
468 testing of chemicals, freshwater alga and cyanobacteria, Growth Inhibition Test. OECD
469 Guideline 201, France.
470 Park, C.M., Wang, D.J., Heo, J., Her, N. & Su, C.M. (2018). Aggregation of reduced graphene oxide
471 and its nanohybrids with magnetite and elemental silver under environmentally relevant
472 conditions. *J Nanopart Res*, 20.
473 Pretti, C., Oliva, M., Di Pietro, R., Monni, G., Cevasco, G., Chiellini, F. *et al.* (2014). Ecotoxicity of
474 pristine graphene to marine organisms. *Ecotox Environ Safe*, 101, 138-145.
475 Ruoff, R.S. & Park, S. (2009). Chemical methods for the production of graphenes. *Nature*
476 *Nanotechnology*, 4, 217.
477 Seda, B.C., Ke, P.C., Mount, A.S. & Klaine, S.J. (2012). Toxicity of aqueous C70-gallic acid
478 suspension in Daphnia magna. *Environ Toxicol Chem*, 31, 215-220.
479 Shim, G., Kim, J.-Y., Han, J., Chung, S.W., Lee, S., Byun, Y. *et al.* (2014). Reduced graphene oxide
480 nanosheets coated with an anti-angiogenic anticancer low-molecular-weight heparin
481 derivative for delivery of anticancer drugs. *Journal of Controlled Release*, 189, 80-89.
482 Souza, J.P., Venturini, F.P., Santos, F. & Zucolotto, V. (2018). Chronic toxicity in Ceriodaphnia dubia
483 induced by graphene oxide. *Chemosphere*, 190, 218-224.
484 Stanley, J.K., Laird, J.G., Kennedy, A.J. & Steevens, J.A. (2016). Sublethal effects of multiwalled
485 carbon nanotube exposure in the invertebrate Daphnia magna. *Environ Toxicol Chem*, 35,
486 200-204.
487 Yang, C., Zhou, J., Liu, S., Fan, P., Wang, W. & Xia, C. (2013). Allelochemical induces growth and
488 photosynthesis inhibition, oxidative damage in marine diatom Phaeodactylum tricornutum.
489 *Journal of Experimental Marine Biology and Ecology*, 444, 16-23.

Zhang, Y, Sun, Q., Zhou, J., Masunaga, S., Ma, F., (2015). Reduction in toxicity of wastewater from three wastewate rtreatment plants to alga (Scenedesmus obliquus) in northeast China. *Ecotoxicology and Environmental Safety*, 119, 132-139.

Zhang, X., Sui, M., Yan, X., Huang, T. & Yuan, Z. (2016). Mitigation in the toxicity of graphene oxide nanosheets towards Escherichia coli in the presence of humic acid. *Environ Sci Process Impacts*, 18, 744-750.

Zhao, J., Cao, X., Wang, Z., Dai, Y. & Xing, B. (2017a). Mechanistic understanding toward the toxicity of graphene-family materials to freshwater algae. *Water research*, 111, 18-27.

Zhao, J., Cao, X.S., Wang, Z.Y., Dai, Y.H. & Xing, B.S. (2017b). Mechanistic understanding toward the toxicity of graphene-family materials to freshwater algae. *Water Res*, 111, 18-27.

Zou, W., Zhou, Q.X., Zhang, X.L., Mu, L. & Hu, X.G. (2018). Characterization of the effects of trace concentrations of graphene oxide on zebrafish larvae through proteomic and standard methods. *Ecotox Environ Safe*, 159, 221-231.

Graphic Abstract